



# Microwave dielectric properties of low-fired $\text{Li}_2\text{TiO}_3\text{-MgO}$ ceramics for LTCC applications

Jian-Li Ma<sup>a</sup>, Zhi-Fen Fu<sup>a,\*</sup>, Peng Liu<sup>b</sup>, Bing Wang<sup>a</sup>, Yang Li<sup>a</sup>

<sup>a</sup> School of Science, Anhui University of Science and Technology, Huainan 232001, China

<sup>b</sup> College of Physics and Information Technology, Shaanxi Normal University, Xi'an 710062, China



## ARTICLE INFO

### Article history:

Received 25 May 2015

Received in revised form

28 September 2015

Accepted 6 October 2015

Available online 27 November 2015

### Keywords:

Ceramics

Microwave dielectric properties

Microstructure

LTCC

## ABSTRACT

We fabricated the low-fired  $\text{Li}_2\text{TiO}_3\text{-MgO}$  ceramics doped with LiF by a conventional solid-state route, and investigated systematically their sintering characteristics, microstructures and microwave dielectric properties. The results showed that temperature stability of  $\text{Li}_2\text{TiO}_3$  ceramics were improved by doping MgO. Well microwave dielectric properties for  $\text{Li}_2\text{TiO}_3\text{-}13\text{ wt%MgO}$  (LTM) ceramics with  $\varepsilon_r = 16.4$ ,  $Q \times f = 87,500$  GHz, and  $\tau_f = -1.2$  ppm/ $^{\circ}\text{C}$  were obtained at  $1325^{\circ}\text{C}$ . Furthermore, addition of LiF enhanced the sinterability and optimized the microwave dielectric properties of LTM ceramics. A typically sample of LTM-4 wt%LiF ceramics with optimum dielectric properties ( $\varepsilon_r = 15.8$ ,  $Q \times f = 64,500$  GHz, and  $\tau_f = -0.2$  ppm/ $^{\circ}\text{C}$ ) were achieved at  $850^{\circ}\text{C}$  for 4 h. Such sample was compatible with Ag electrodes, suitable for the low-temperature co-fired ceramics (LTCC) applications.

© 2015 Elsevier B.V. All rights reserved.

## 1. Introduction

With the rapid development of modern microwave communication systems, high-quality microwave dielectric ceramics have attracted increasing research due to their potential application in mobile and satellite communication. Nowadays, the low-temperature co-fired ceramic (LTCC) applications has aroused considerable attention due to its advantage in enabling the fabrication of miniature modules by integrating electronic components and devices in a compact multilayer ceramic structure. The microwave dielectric materials used in LTCC field should have appropriate dielectric constant ( $\varepsilon_r$ ), high  $Q \times f$  value ( $Q \times f \geq 5000$  GHz), a near-zero temperature coefficient of resonant frequency ( $\tau_f$ ), and co-fired with metal electrodes, such as Ag, Cu. Therefore, the lowering of the sintering temperature of ceramics would also have an ecological and economic impact due to a reduced consumption of electrical energy.

Recently, lithium based oxide ceramics  $\text{Li}_2\text{MO}_3$  ( $M = \text{Ti}, \text{Zr}, \text{Sn}$ ),  $\text{Li}_3\text{MO}_4$  ( $M = \text{Sb}, \text{Ta}$ ), and  $\text{Li}_2\text{ATi}_3\text{O}_8$  ( $A = \text{Mg}, \text{Zn}$ ) are very attractive subjects for materials research and engineering applications [1–3]. Among them, rock salt structure of  $\text{Li}_2\text{TiO}_3$  ceramic received special attention due to its good dielectric properties:  $\varepsilon_r \sim 22$ ,  $Q \times f$  above 15,525 GHz, and  $\tau_f = 20\text{--}38$  ppm/ $^{\circ}\text{C}$  [4]. However, its  $\tau_f$  value is a

little large and sintering temperatures (around  $1200^{\circ}\text{C}$ ) is too high to apply in LTCC. By forming a solid solution with MgO or ZnO, the quality factor of  $\text{Li}_2\text{TiO}_3$  could be improved to about 100,000 GHz and a near-zero temperature coefficient of resonant frequency for  $0.7\text{Li}_2\text{TiO}_3\text{-}0.3\text{MgO}$  (ZnO) ceramics could also be obtained [5,6]. However, the high sintering temperature ( $1300\text{--}1325^{\circ}\text{C}$ ) and the porous microstructure of  $\text{Li}_2\text{TiO}_3$  based ceramics hindered their practical applications. In order to lower the sintering temperature, ultrafine nanopowders and glass frits such as  $\text{H}_3\text{BO}_3$ , and  $\text{B}_2\text{O}_3\text{-CuO}$  were usual used [1,7,8]. But the glassy phase with higher dielectric loss could be detrimental to the further enhancement of microwave dielectric properties. According to our previously work,  $\text{Li}_2\text{TiO}_3$  ceramics were prepared at low temperature ( $1000^{\circ}\text{C}$ ) by using low temperature synthesis nanopowders as a precursor [9]. Low melting fluorides such as LiF were reported to be effective as sintering flux in several microwave ceramic systems [10–13].

In this paper, we used MgO as an  $\tau_f$  compensator and LiF as sintering aid for  $\text{Li}_2\text{TiO}_3$  ceramics. The effects of MgO and LiF on the sintering characteristics, microstructures and microwave dielectric properties of  $\text{Li}_2\text{TiO}_3$  ceramics were studied systematically, and found that the sinterability was enhanced and the microwave dielectric properties were optimized.

## 2. Experimental procedure

The  $\text{Li}_2\text{TiO}_3\text{-}13\text{ wt%MgO}\text{-(0-6 wt%)LiF}$  ceramics were prepared by a conventional solid-state route.  $\text{Li}_2\text{CO}_3$  (98%, Guo-Yao Co. Ltd.,

\* Corresponding authors.

E-mail address: [fuzhifen80@sina.com](mailto:fuzhifen80@sina.com) (Z.-F. Fu).

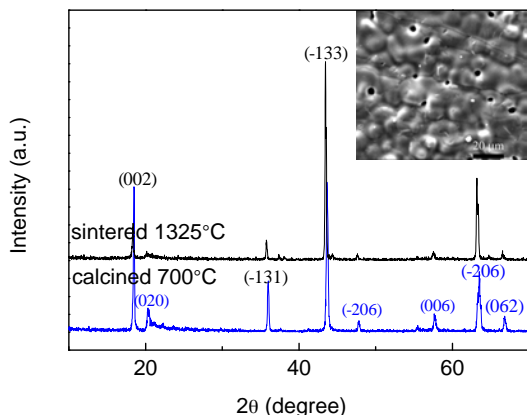


**Fig. 1.** The XRD pattern of the  $\text{Li}_2\text{TiO}_3$  powders calcined at  $700^\circ\text{C}$ , and the XRD pattern and SEM image of the LTM ceramics sintered at  $1325^\circ\text{C}$ .

Shanghai, China),  $\text{TiO}_2$  (99.99%, Guo-Yao Co. Ltd., Shanghai, China),  $\text{MgO}$  (99.99%, Guo-Yao Co. Ltd., Shanghai, China) and  $\text{LiF}$  (99.6%, Zhong-li Co. Ltd., Shanghai, China) powders were used as starting materials. Stoichiometric  $\text{Li}_2\text{CO}_3$  and  $\text{TiO}_2$  (total powders of 20 g) were mixed according to the formula of  $\text{Li}_2\text{TiO}_3$  milled with  $\text{ZrO}_2$  balls in ethanol (40 ml) for 8 h. Then the mixtures were dried and calcined at  $700^\circ\text{C}$  for 5 h in air. The obtained  $\text{Li}_2\text{TiO}_3$ ,  $\text{MgO}$  and  $\text{LiF}$  powders were weighed according to the designed molar ratios, ball-milled for 8 h, dried and sieved. Required the total powder to Ball wt% ratio is 1:20, and the size of the ball is 6 mm (twenty), 10 mm (ten) and 20 mm (two), respectively. Subsequently, the powders (the particle size at a scale of 4–10  $\mu\text{m}$ ) were granulated with 5 wt% PVA as binder and uniaxially pressed into cylindrical disks (11.5 mm in diameter and about 6 mm in height) under a pressure of 98 MPa. These pellets were sintered at  $800\text{--}1350^\circ\text{C}$  for 4 h on alumina plates at a heating rate of  $4^\circ\text{C}/\text{min}$ .

The bulk densities of the sintered ceramics were measured by Archimedes method. The crystal structures were analyzed using X-ray diffraction (XRD) with  $\text{Cu K}_\alpha$  radiation (Rigaku D/MAX2550, Tokyo, Japan). The Raman spectra (RENISHAW in Via plus, UK) were excited with the 532 nm line of a semiconductor laser at a power of 250 mW and recorded in back-scattering geometry using In Via Raman Microscope equipped with a grating filter, enabling good stray light rejection in the  $100\text{--}1000\text{ cm}^{-1}$  range. The microstructures were investigated using a scanning electron microscope (SEM, Quanta 200, FEI Company, Eindhoven, Holland) coupled with energy dispersive X-ray spectroscopy (EDS). The microwave dielectric properties of the specimens were measured using a network analyzer (ZVB20, Rohde & Schwarz, Munich, Germany) with the TE<sub>018</sub> shielded cavity method. The temperature coefficient resonant frequency ( $\tau_f$ ) was calculated with the following formula:

$$\tau_f = \frac{(f_2 - f_1) \times 10^6}{f_1(T_2 - T_1)} \quad (1)$$

where  $f_2$  and  $f_1$  represent the resonant frequency at  $T_2$  and  $T_1$ , respectively.  $T_1$  and  $T_2$  are  $20^\circ\text{C}$  and  $80^\circ\text{C}$ , respectively.

**Table 1**

The density and microwave dielectric properties of LTM ceramics.

S.T. ( $^\circ\text{C}$ )	Bulk density ( $\text{g}/\text{cm}^3$ )	Relative density	$\varepsilon_r$	$Q \times f (\text{GHz})$	$\tau_f (\text{ppm}/^\circ\text{C})$
1250	3.05	87.9	15.2	71,800	2.1
1275	3.22	92.8	15.8	79,100	1.9
1300	3.24	93.3	16.1	84,300	1.8
1325	3.27	94.2	16.4	87,500	-1.2
1350	3.20	92.3	16.8	74,300	-2.3

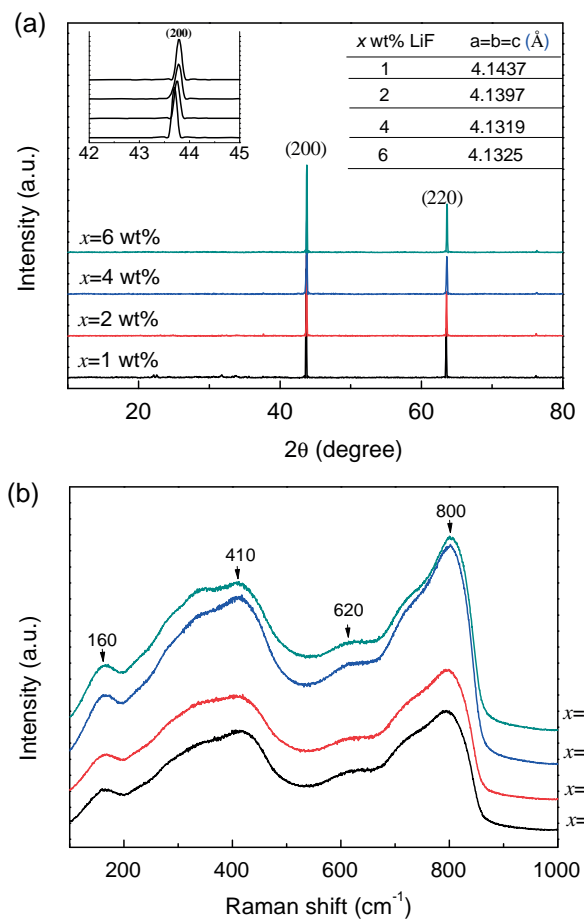


**Fig. 2.** (a) XRD patterns and (b) Raman spectra of  $x$  wt%  $\text{LiF}$ -doped LTM ceramics sintered at  $850^\circ\text{C}$  as function of  $x$ . Inset of (a) is the profiles of (200) reflections and variation of the lattice constant of  $\text{Li}_2\text{TiO}_3$ .

### 3. Results and discussions

#### 3.1. $\text{Li}_2\text{TiO}_3\text{--MgO}$ system

Fig. 1 shows the XRD pattern of the  $\text{Li}_2\text{TiO}_3$  powders calcined at  $700^\circ\text{C}$ , and the XRD pattern and SEM image of  $\text{Li}_2\text{TiO}_3\text{--}13$  wt%  $\text{MgO}$  (LTM) ceramic sintered at  $1325^\circ\text{C}$ . The XRD pattern displays monoclinic structure ( $\beta\text{-Li}_2\text{TiO}_3$  (ss), PDF# 33-0831) and no additional peaks are observed. The SEM image exhibits porous microstructure due to the volatilization of Li in the high temperature, the similar phenomenon was observed in Ref. [5]. Table 1 gives bulk density and microwave dielectric properties of LTM ceramics sintered at various temperatures. Bulk density increases with an increase in sintering temperatures, reaches a maximum ( $3.27\text{ g}/\text{cm}^3$ ) at  $1325^\circ\text{C}$ , and then decreased with a further increasing temperature.

Compared with  $\text{Li}_2\text{TiO}_3$  ceramics, the higher densification temperature of  $\text{MgO}$ -doped ceramics was associated with the higher melting point of  $\text{MgO}$  [14]. The variation in  $\varepsilon_r$  and  $Q \times f$  values with sintering temperatures is consistent with that of bulk density

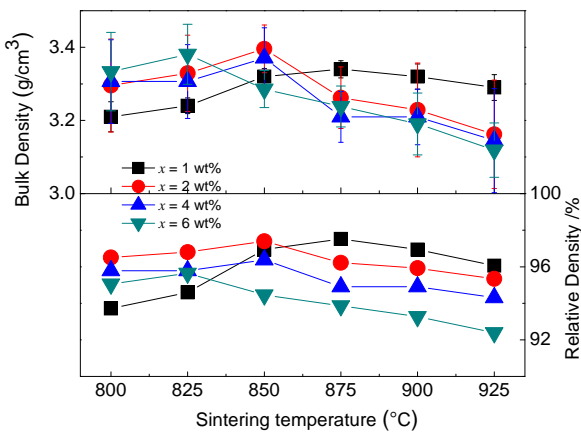


**Fig. 3.** The density of LTM ceramics doped with  $x$  wt% LiF as functions of sintering temperatures and  $x$  (including  $\pm 3\%$  error bars).

with sintering temperatures, which suggests that the density is the dominating factor to control  $\varepsilon_r$  and  $Q \times f$  values in  $\text{Li}_2\text{TiO}_3\text{-MgO}$  ceramics. The  $\tau_f$  values of the samples decreased from 2.1 to  $-2.3 \text{ ppm}/^\circ\text{C}$  continuously with increasing sintering temperatures. A well dielectric properties of  $\varepsilon_r \sim 16.4$ ,  $Q \times f \sim 87,500 \text{ GHz}$ , and  $\tau_f = -1.2 \text{ ppm}/^\circ\text{C}$  is obtained for LTM samples sintered at  $1325^\circ\text{C}$  for 4 h, which is similar to reported in  $\text{Li}_2\text{TiO}_3\text{-MgO}$  [5].

### 3.2. $\text{Li}_2\text{TiO}_3\text{-MgO-LiF}$ system

In order to decrease sintering temperatures to less than  $950^\circ\text{C}$  for LTCC applications, LiF powders were added into LTM matrix.

**Fig. 2(a)** presents the XRD patterns of LiF-doped LTM ceramics sintered at  $850^\circ\text{C}$ . The XRD patterns exhibit disordered cubic phase ( $\alpha\text{-Li}_2\text{TiO}_3$  (ss), PDF# 03-1024), the similar transform of ordered monoclinic phase into disordered cubic phase was observed in  $\text{Li}_2\text{TiO}_3\text{-LiF}$  system [15]. No additional phases are detected. In the insert of **Fig. 2(a)**, with increasing of LiF content, the intensity of (2 0 0) peak decreases implying that the disordering degree decreased. Furthermore, the peaks of (2 0 0) shift toward to a higher angle suggesting that the lattices constant of  $\text{Li}_2\text{TiO}_3$  decreases with increasing of LiF content ( $x$ ). It was reported that the LiF liquid phase is transient and would form substitutional solid solution with  $\text{Li}_2\text{TiO}_3$  after sintering at  $875^\circ\text{C}$  when content of LiF  $< 0.2 \text{ mol\%}$  (equivalently 5.2 wt%) [15]. So, the decreasing of lattices constant might be owing to the substitution of the  $\text{F}^-$  ion ( $R = 1.33 \text{ \AA}$ ) for  $\text{O}^{2-}$  ( $R = 1.4 \text{ \AA}$ ) sites, agreeing with Ref. [10]. The replacement mechanisms as following:



According to Eq. (2), three  $\text{F}^-$  anions and one  $\text{Li}^+$  ( $R = 0.76 \text{ \AA}$ ) replaced three  $\text{O}^{2-}$  and one  $\text{Ti}^{4+}$  ( $R = 0.605 \text{ \AA}$ ), respectively, resulting in lattice contraction. While LiF addition  $> 6 \text{ wt\%}$ , the lattices constant decrease, which is associated with that a large extent of liquid phase during sintering process inhibit the entrance or occupation of  $\text{Li}^+$  and  $\text{F}^-$  in the  $\text{Li}_2\text{TiO}_3$  lattice. Thus, just small amounts of  $\text{F}^-$  can be incorporated into  $\text{Li}_2\text{TiO}_3$  lattice and the solid solubility limit of  $\text{F}^-$  in  $\text{Li}_2\text{TiO}_3$  is about 4 wt%. Raman spectroscopy is more suitable than XRD to detect the local structure. **Fig. 2(b)** gives the Raman spectra of LiF-doped LTM ceramics sintered at  $850^\circ\text{C}$ . All spectra exhibit similar Raman spectra at  $160 \text{ cm}^{-1}$ ,  $410 \text{ cm}^{-1}$ ,  $620 \text{ cm}^{-1}$  and  $800 \text{ cm}^{-1}$ . With increasing LiF content, the increase in intensity

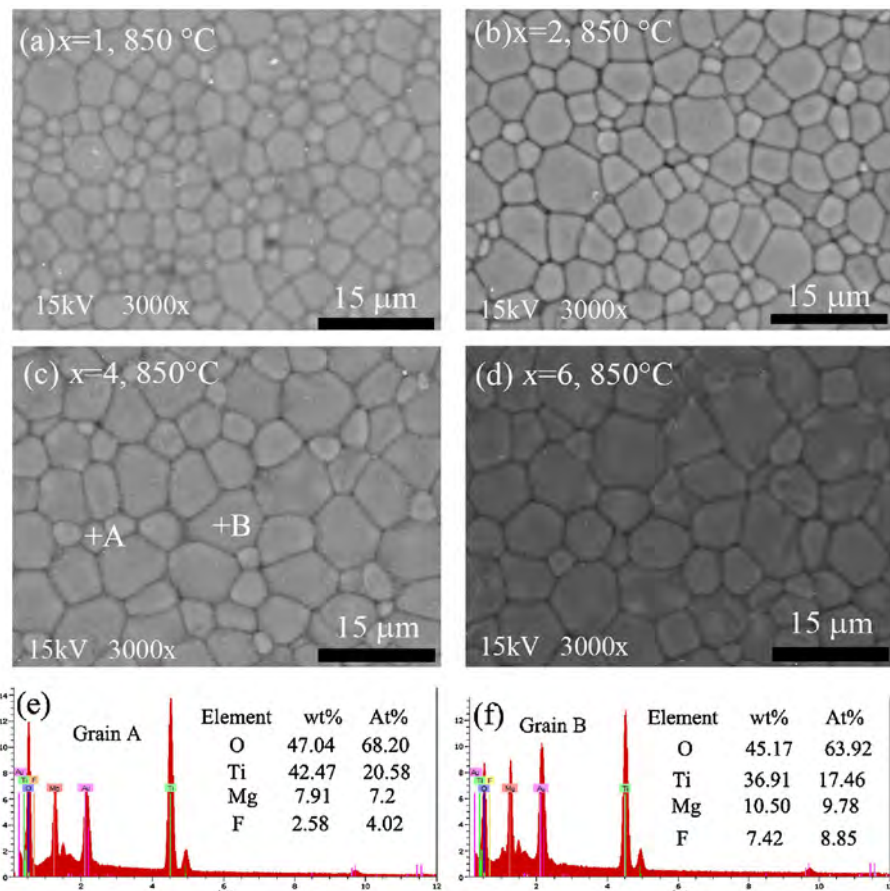


**Fig. 4.** (a-d) SEM images of  $x$  wt% LiF doped LTM ceramics sintered at  $850^\circ\text{C}$  as function of  $x$ , and (e-f) the EDS datum of grain A and B.

of the Raman bands near  $160\text{ cm}^{-1}$  and  $800\text{ cm}^{-1}$  reveal that the disordering degree decreased with the increase of LiF content, which is in well agreement with that observed by XRD (Fig. 2(a)).

Fig. 3 summarizes bulk density of LiF-doped LTM ceramics as functions of sintering temperatures and  $x$ . The error is derived from the mean standard deviation and the error bars are plotted in Fig. 3. It can be seen that the densities increase with increasing sintering temperatures and then decrease after reaching their respective maximum values. Bulk density of specimens ( $x \leq 4$ ) sintered at  $825\text{--}875\text{ }^\circ\text{C}$  are all above  $3.27 \pm 0.02\text{ g/cm}^3$  (relative density of 96%), which is higher than those of pure LTM ceramics (relative density of 94%, Table 1). However, density decreases as increasing  $x$ , due to lower theoretical density of LiF ( $2.64\text{ g/cm}^3$ ) than that of  $\text{Li}_2\text{TiO}_3$  ( $3.42\text{ g/cm}^3$ ). The densification temperature of sintered ceramics tends to decrease from  $875\text{ }^\circ\text{C}$  to  $825\text{ }^\circ\text{C}$  with increasing  $x$  from 1 to 6. It was obvious that additions LiF can not only successfully reduce sintering temperatures to below  $875\text{ }^\circ\text{C}$  but also improve densification.

The SEM images of LiF-doped LTM ceramics sintered at  $850\text{ }^\circ\text{C}$  are illustrated in Fig. 4(a)–(d). Compared with LTM ceramics (Fig. 1), it can be seen that LiF-doped LTM specimens show well-dense microstructure at  $850\text{ }^\circ\text{C}$ , which further confirmed the effectiveness of LiF in promoting the sintering behavior of  $\text{Li}_2\text{TiO}_3\text{--MgO}$  ceramics. With increasing  $x$ , the average grain size increases because of the elevated boundary diffusion coefficient. Furthermore, as shown in Fig. 4(e) and (f), a remarkable difference could be observed from the EDS analysis for the grains marked A and B. Compared with the grain A, the grain B shows much more content of F, indicating  $\text{F}^-$  ion can effectively promote grain growth. Two plausible explanations for this phenomenon are proposed here. One is that liquid phase is formed during the sintering process due to the lower melting point of LiF ( $845\text{ }^\circ\text{C}$ ). The presence of liquid phase significantly enhances the particle rearrangement and the mass transport by solution-precipitation. The other is that, the crystal defect induced by the substitution of smaller  $\text{F}^-$  for  $\text{O}^{2-}$ , as evidenced by XRD analysis, causes weakening of oxygen bond strength, which facilitates the diffusion process and thus reduces the intrinsic sintering temperatures. Since the  $\text{F}^-$  ion has a lower bonding energy and smaller ion radius compared with  $\text{O}^{2-}$ . The accurate determination of  $\text{F}^-$  ion occupation in the lattice which is crucial to the investigation of defects and grain growth deems necessary in the future.

Fig. 5(a–c) demonstrates microwave dielectric properties of samples sintered at various temperatures as functions of LiF additions. The error is derived from the mean standard deviation and the error bars are plotted in Fig. 5. As shown in Fig. 5(a), the variations in  $\varepsilon_r$  with sintering temperatures and  $x$  are consistent with that of bulk density, suggests that the density is the dominating factor to control  $\varepsilon_r$  in  $\text{Li}_2\text{TiO}_3\text{--MgO}$  ceramics. The dielectric constant of ceramic material is predominantly decided by the dipoles in unit cell volume and dielectric polarizabilities of ions [16]. To be specific, higher density exhibits higher  $\varepsilon_r$  value as a result of more dipoles and more apt to be polarized. Furthermore, the  $\varepsilon_r$  could be calculated according to the Clausius–Mossotti equation [16]:

$$\varepsilon_r = \frac{3V_m + 8\pi\alpha_D}{3V_m + 4\pi\alpha_D} \quad (3)$$

where  $V_m$  is the molar volume and  $\alpha_D$  is the sum of the dielectric polarizabilities of individual ions. In the  $\text{Li}_2\text{TiO}_3\text{--MgO}$ –LiF system, the substitution of  $\text{F}^-$  for  $\text{O}^{2-}$ , and  $\text{Li}^+$  for  $\text{Ti}^{4+}$  would decrease  $\alpha_D$  considering their relative polarizabilities [ $\alpha(\text{F}^-) = 1.62\text{ \AA}^3$ ,  $\alpha(\text{Li}^+) = 1.2\text{ \AA}^3$ ,  $\alpha(\text{O}^{2-}) = 2.01\text{ \AA}^3$ ,  $\alpha(\text{Ti}^{4+}) = 2.93\text{ \AA}^3$ ]. Thus, as illustrated in Fig. 5(a), the  $\varepsilon_r$  values decrease from 16.0 to 15.6 as increasing  $x$  due to the comparative lower dielectric polarizabilities of  $\text{F}^-$  and  $\text{Li}^+$  than that of  $\text{O}^{2-}$  and  $\text{Ti}^{4+}$ , respectively. In Fig. 5(b), with increasing sintering temperatures and  $x$ ,  $Q \times f$  values increases and reaches a maximum value of  $64,500\text{ GHz}$  at  $850\text{ }^\circ\text{C}$ .

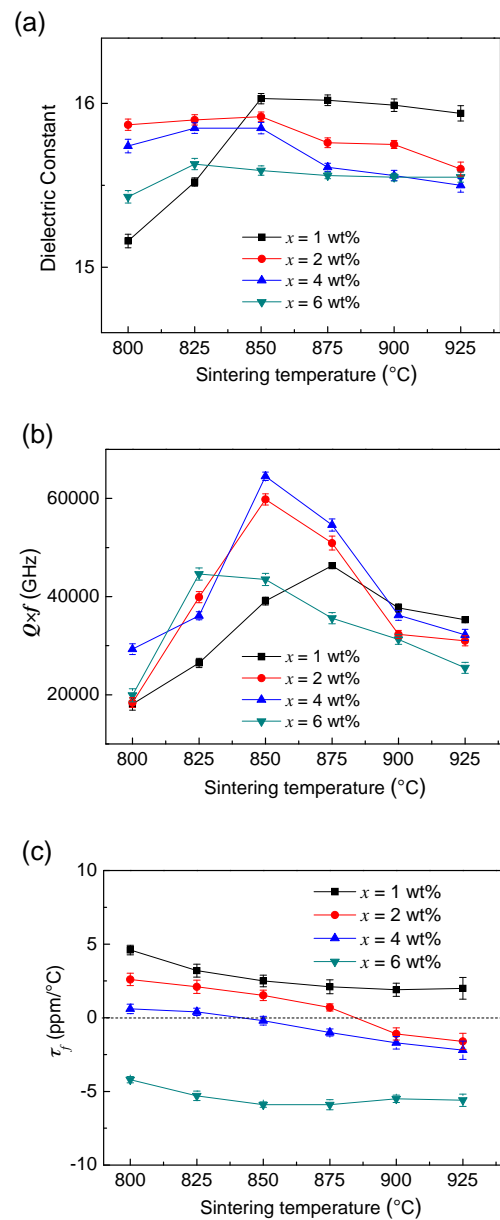
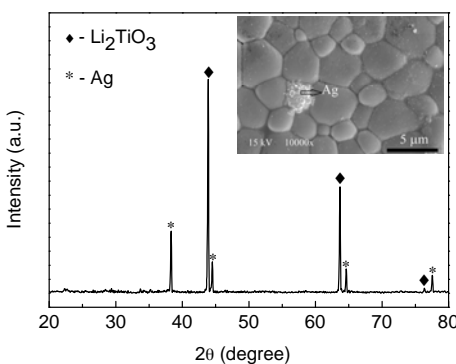


Fig. 5. Variation of microwave dielectric properties of  $x$  wt% LiF-doped LTM ceramics sintered at various temperatures with different LiF contents (including  $\pm 2\%$  error bars).

for sample ( $x=4$ ), and then decreases. It is well known that dielectric loss is mainly caused not only by the lattice vibration modes, but also by impurities, second phase, pores, lattice defect, and grain boundary or grain morphology [17]. For slight amount of LiF doped samples, the increasing of  $Q \times f$  values with increasing  $x$  was associated with uniform microstructures and a range of small grain sizes with a narrow distribution. In general,  $\tau_f$  is well known to be influenced by the composition, the additive and the second phase of the materials [18]. It can be seen in Fig. 5(c), the  $\tau_f$  value shows a continuous negative increase in magnitude as increasing LiF content. Through appropriate adjustment, a  $-0.2\text{ ppm/}^\circ\text{C}$  of  $\tau_f$  can be obtained for LTM-4 wt% LiF specimen sintered at  $850\text{ }^\circ\text{C}$ .

Fig. 6 presents the XRD pattern and SEM image of LTM-4 wt% LiF ceramics doped with 10 wt% silver (Ag) powders and sintered at  $850\text{ }^\circ\text{C}$  for 2 h. As is seen in Fig. 6, for the co-fired sample, only the peaks of  $\text{Li}_2\text{TiO}_3$  phase and the respective metals (Ag) are observed. No additional peaks in the XRD patterns can be detected, implying



**Fig. 6.** The XRD pattern and SEM image of the LTM-4 wt% LiF ceramics doped with 10 wt% Ag powders sintered at 850 °C for 2 h.

that LTM composite ceramic does not react with Ag powder at 850 °C for 2 h. According to this, LiF doped LTM ceramics could be selected as suitable candidates for LTCC applications.

#### 4. Conclusions

In this paper, the sintering characteristics, microstructures, and microwave dielectric properties of  $\text{Li}_2\text{TiO}_3$ – $\text{MgO}$  ceramics doped with LiF were studied. The temperature stability of  $\text{Li}_2\text{TiO}_3$  ceramics were improved by  $\text{MgO}$  additions, and a well microwave dielectric properties ( $\varepsilon_r = 16.4$ ,  $Q \times f = 87,500 \text{ GHz}$ , and  $\tau_f = -1.2 \text{ ppm}/^\circ\text{C}$ ) for LTM samples were obtained at 1325 °C. Furthermore, addition of LiF successfully reduced sintering temperatures to below 875 °C and optimized the microwave dielectric properties. 4 wt% LiF doped LTM ceramics sintered at 850 °C exhibited the best microwave dielectric properties:  $\varepsilon_r = 15.8$ ,  $Q \times f = 64,500 \text{ GHz}$ ,  $\tau_f = -0.2 \text{ ppm}/^\circ\text{C}$ . In addition, the chemical compatibilities of 4 wt% LiF doped

composition with Ag powders were also investigated. No chemical reaction has taken place among the LTM-4 wt% LiF matrix and Ag powders after co-fired at 850 °C for 2 h. The low-temperature sintering ceramics powders are suitable for the LTCC applications.

#### Acknowledgments

This work was supported by the National Natural Science Foundation of China (grant no. 51502005), Anhui Provincial Natural Science Foundation (grant no. 1408085QA11), the Master/Doctor Foundation of Anhui University of Science and Technology (grant no. 111143), and the Young Teachers Scientific Research Foundation of Anhui University of Science and Technology (grant no. QN201427).

#### References

- [1] L.X. Pang, D. Zhou, J. Am. Ceram. Soc. 93 (2010) 3614–3617.
- [2] L.X. Pang, H. Liu, D. Zhou, et al., J. Alloys Compd. 525 (2012) 22–24.
- [3] S. George, M.T. Sebastian, J. Am. Ceram. Soc. 93 (2010) 2164–2166.
- [4] L.L. Yuan, J.J. Bian, Ferroelectrics 38 (2009) 123–129.
- [5] J.J. Bian, Y.F. Dong, J. Eur. Ceram. Soc. 30 (2010) 325–330.
- [6] C.L. Huang, Y.W. Tseng, J.Y. Chen, J. Eur. Ceram. Soc. 32 (2012) 3287–3295.
- [7] Y. Li, C.L. Wu, W.Z. Huang, et al., J. Anhui Univ. Sci. Technol.: Nat. Sci. Ed. 26 (2006) 41–44.
- [8] J. Liang, W.Z. Lu, J.M. Wu, et al., Mater. Sci. Eng., B 176 (2011) 99–102.
- [9] Z.F. Fu, P. Liu, J.L. Ma, Mater. Sci. Eng., B 193 (2015) 32–36.
- [10] Y.Z. Hao, H. Yang, G.H. Chen, et al., J. Alloys Compd. 525 (2013) 173–179.
- [11] N.X. Xu, J.H. Zhou, H. Yang, Ceram. Int. 40 (2014) 15191–15198.
- [12] S.F. Wang, T.C.K. Yang, W. Huebner, et al., J. Mater. Res. 15 (2000) 407–416.
- [13] U. Intathra, S. Eitssayeam, K. Pengpat, et al., Mater. Lett. 61 (2007) 196–200.
- [14] Y.J. Wei, H.X. Li, J. Anhui Univ. Sci. Technol.: Nat. Sci. Ed. 28 (2008) 74–77.
- [15] Y.M. Ding, J.J. Bian, Mater. Res. Bull. 48 (2013) 2776–2781.
- [16] M.T. Sebastian, Dielectric Materials for Wireless Communication, Elsevier, Amsterdam, 2010.
- [17] B.D. Silverman, Phys. Rev. 15 (1962) 1921–1930.
- [18] C.L. Huang, S.H. Liu, J. Am. Ceram. Soc. 91 (2008) 3428–3430.